Electronic Supplementary Information For

Preprogrammed capillarity to passively control system-level sequential and pa rallel microfluidic flows

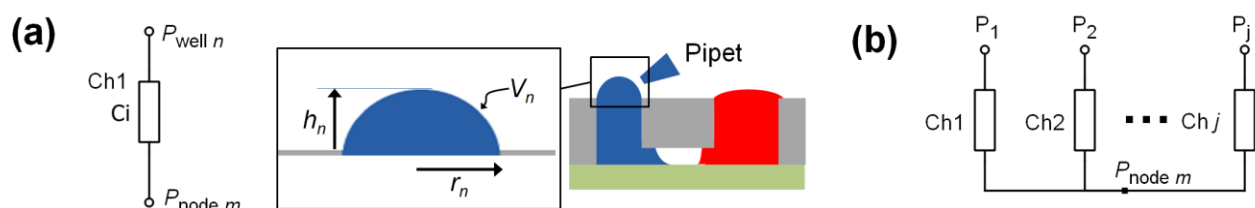Sung-Jin Kim, Sophie Paczesny, Shuichi Takayama, Katsuo Kurabayashi

Fig. S1. (a) Diagram showing $P_{\text{well } n}$ and node pressure ($P_{\text{node } m}$). The difference between $P_{\text{well } n}$ and $P_{\text{node } m}$ drives a flow. The node-to-well volume flow rate $Q_{\text{node}\rightarrow\text{well}} = C_i (P_{\text{node } m} - P_{\text{well } n})$ is equal to the increasing rate of the liquid drop volume $\frac{dV_n}{dt} = \frac{\pi(r_n{}^2 + h_n{}^2)}{2}\frac{dh_n}{dt}$, where V_n is the volume of the convex drop in the well n, and r_n and h_n are the well radius and the drop height, respectively. Thus, $\frac{dh_n}{dt} = \frac{2C_i(P_{\text{node } m} - P_{\text{well } n})}{\pi(r_n{}^2 + h_n{}^2)}$. $P_{\text{well } n}$ is determined by the drop shape as $P_{\text{well } n} = \frac{4\sigma h_n}{h_n{}^2 + r_n{}^2}$, where σ is the surface tension of the drop. (b) Diagram for $P_{\text{node } m}$. Analogous to Kirchhoff's current law, the sum of the volume flow rates coming into node m is 0. That is, $\sum_{i=1}^{j} C_i (P_{\text{node } m} - P_i) = 0$, where P_i is either well or another node pressure. Thus, $P_{\text{node } m}$ is $\frac{\sum_{i=1}^{j} C_i P_i}{\sum_{i=1}^{j} C_i}$. The two types of equations for $\frac{dh_n}{dt}$ and $P_{\text{node } m}$ constitute simultaneous differential equations of the entire fluidic network, and they are solved numerically (MATLAB, Mathworks).
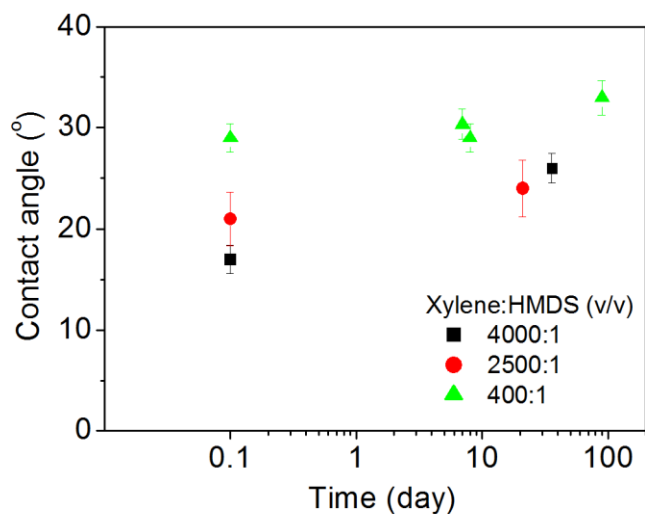
Fig. S2. Adjustment of contact angle for the device bottom layer. The contact angle was measured on surface-treated silicon for phosphate buffered saline (PBS) solution. The results show that the surface coated with the xylene-to-HMDS ratio of 400:1 was hydrophilically stable and maintained an appropriate contact angle value, which did not result in the edge wetting of a channel cross-section. Thus, we used the surface for the device.
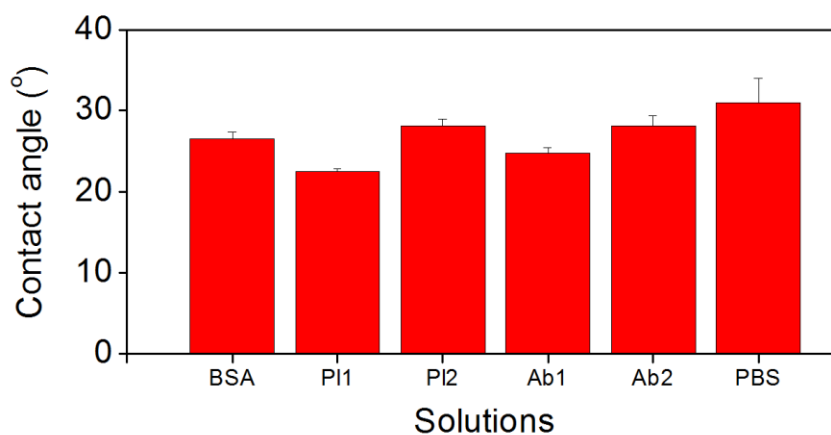

Figure S3. Contact angles of various immunoassay solutions on a stable hydrophilic surface (xylene : HMDS = 400:1). Each solution was measured in triplicate. Pl1 and Pl2 were human plasmas from different donors. Ab1 and Ab2 are 6.7 μM C-reactive protein (CRP) antibody and 600 nM FITC-labeled CRP antibody (Bethyl Laboratory), respectively
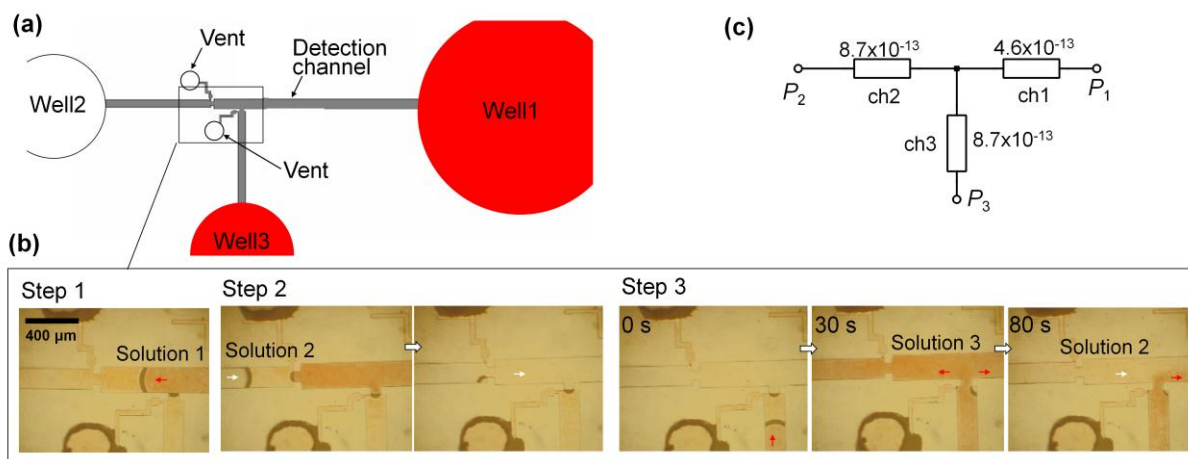
Fig. S4. Disturbance of sequential flows. (a) Schematic of 3-well system. (b) Photographs of sequential flows. Solutions 1, 2, and 3 were sequentially dispensed in wells 1, 2, and 3, respectively, and their initial well pressures (P_1, P_2, and P_3) were 7, 127 and 127 Pa, respectively. In step 3, solution 3 was dispensed in well 3 after P_1 and P_2 equilibrated. Note that solution 2 reflowed in step 3. (c) Fluidic circuit diagram of step 3 of (b). Each channel's (ch i) fluidic conductance (unit: $m^5\,N^{-1}\,s^{-1}$) is shown in the diagram.
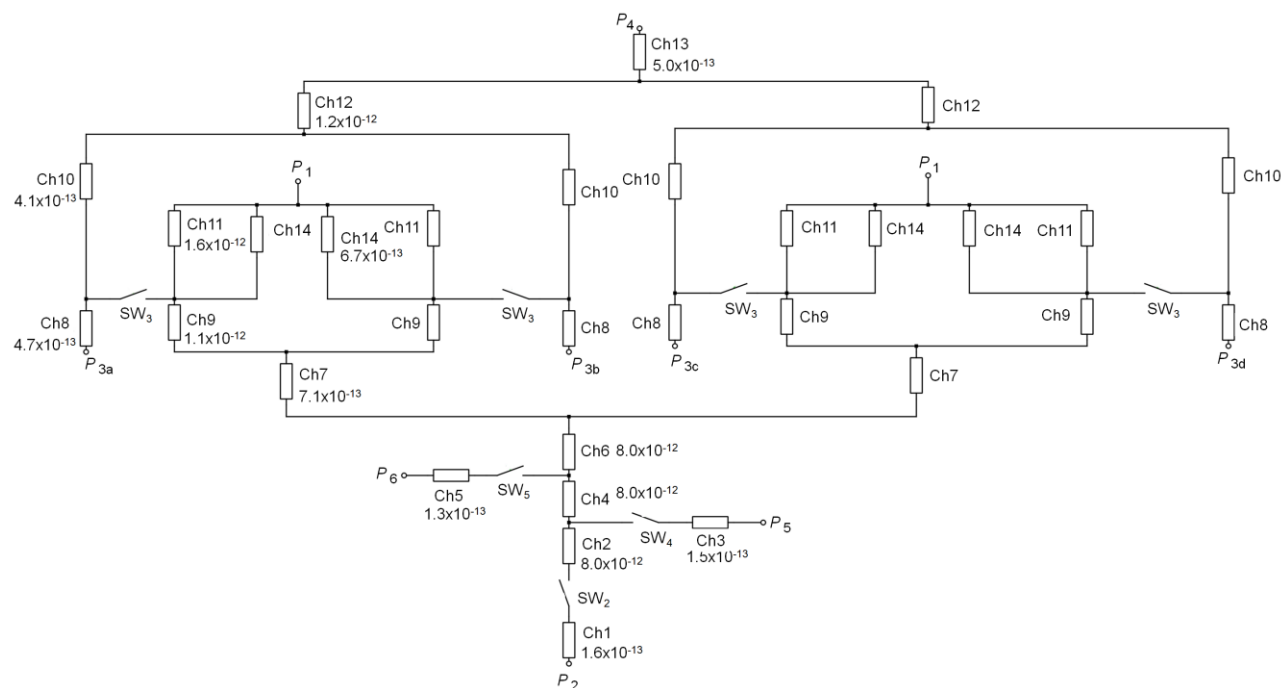

Fig. S5. Microfluidic circuit diagram showing entire fluidic network. The model includes well pressures (P_i) and fluidic channels (Ch i). Each channel's fluidic conductance (unit: $m^5\,N^{-1}\,s^{-1}$), which is

the inverse of fluidic resistance, is noted in the diagram. In the kth step, a solution in an inlet well starts to flow upon turning on the corresponding switch (SW_k) by a timing channel.